G.V. Nikiforovich
B. Mihalik
K.J. Catt
G.R. Marshall

Molecular mechanisms of constitutive activity: mutations at position 111 of the angiotensin AT_1 receptor

Authors' affiliations:
G.V. Nikiforovich and G.R. Marshall, Department of Biochemistry and Molecular Biophysics, Washington University School of Medicine, St Louis, MO 63110, USA

B. Mihalik and K. J. Catt, Endocrinology and Reproduction Research Branch, National Institute of Child Health and Human Development, Bethesda, MD 20892, USA.

Correspondence to:
G.V. Nikiforovich
Department of Biochemistry and Molecular Biophysics
Washington University School of Medicine
St Louis
MO 63110
USA
Tel.: (314) 362-1566
Fax: (314) 362-0234
E-mail: gregory@ccb.wustl.edu

Dates:
Received 27 July 2005
Accepted 23 August 2005

To cite this article:
Nikiforovich, G.V., Mihalik, B., Catt, K.J. & Marshall, G.R. Molecular mechanisms of constitutive activity: mutations at position 111 of the angiotensin AT_1 receptor. *J. Peptide Res.*, 2005, **66**, 236–248.
DOI 10.1111/j.1399-3011.2005.00293.x

Key words: angiotensin; angiotensin type 1 receptor; constitutively active mutants; molecular modeling

Abstract: A possible molecular mechanism for the constitutive activity of mutants of the angiotensin type 1 receptor (AT_1) at position 111 was suggested by molecular modeling. This involves a cascade of conformational changes in spatial positions of side chains along transmembrane helix (TM3) from L112 to Y113 to F117, which in turn, results in conformational changes in TM4 (residues I152 and M155) leading to the movement of TM4 as a whole. The mechanism is consistent with the available data of site-directed mutagenesis, as well as with correct predictions of constitutive activity of mutants L112F and L112C. It was also predicted that the double mutant N111G/L112A might possess basal constitutive activity comparable with that of the N111G mutant, whereas the double mutants N111G/Y113A, N111G/F117A, and N111G/I152A would have lower levels of basal activity. Experimental studies of the above double mutants showed significant constitutive activity of N111G/L112A and N111G/F117A. The basal activity of N111G/I152A was higher than expected, and that of N111G/Y113A was not determined due to poor expression of the mutant. The proposed mechanism of constitutive activity of the AT_1 receptor reveals a novel nonsimplistic view on the general problem of constitutive activity, and clearly demonstrates the inherent complexity of the process of G protein-coupled receptor (GPCR) activation.

Abbreviations: GPCR, G protein-coupled receptor; AT_1, angiotensin receptor type 1; CAM, constitutively active mutant; TM, transmembrane or transmembrane helix; 3D, three-dimensional; IP or Ins, inositol phosphate; IC, intracellular. Both single and three-letter abbreviations are used for amino acid residues

Introduction

G protein-coupled receptors (GPCRs) comprise a vast protein family involved in a wide variety of physiologic functions (e.g. 1), and represent the majority of known targets for currently available drugs (2). Agonist-binding activates GPCRs, i.e. triggers their interactions with their corresponding intracellular (IC)-G proteins. Some mutant GPCRs display constitutive activity, i.e. ligand-independent activity that produces a second messenger even in the absence of an agonist (3). Constitutively active mutants (CAMs) are known for many GPCRs, including rhodopsin, α_{1B}-adrenergic receptor, β_2-adrenergic receptor, angiotensin receptor type I (the AT_1 receptor, AT_1), opioid, cholecystokinin receptors, and many others (see review, for example, Ref. 3). As activation of a GPCR is believed to require conformational changes to trigger interaction with a G protein, it is generally assumed that conformations of CAMs can mimic the active conformations of GPCRs. This assumption is the main rationale for the present study. Obviously, knowledge of the structural mechanisms of GPCR's activation at the molecular level would tremendously benefit the fields of molecular biophysics and pharmacology, and especially impact drug design.

The AT_1 receptor, a 359-residue seven-transmembrane (TM) domain GPCR, is one of the most studied GPCRs by site-directed mutagenesis (4–37). Several researchers have proposed a variety of structural models to describe the differences between the resting and activated states of the AT_1 receptor, based on molecular modeling and/or mutagenesis studies (10,21,23,35,38–43; see also reviews in Ref. 21,44). Early models presumed that, in the inactive state, the side chain of Y292 forms a hydrogen bond with the side chain of N111 [or with the side chain of N295 (35)], which switches to a hydrogen bond with the side chain of D74 in the active state (15,39). Such models were derived from the X-ray structure of bacteriorhodopsin (45), a seven-TM protein that is not a GPCR and has little, if any, homology to the AT_1 receptor sequence.

In models based on the X-ray structure of rhodopsin (46), a GPCR highly homologous to the AT_1 receptor, interactions Y292–D74 are implausible. Besides, more recent data on mutagenesis were interpreted as contradictory to the early models, because various mutations in positions 292 and 295 produced mutants pharmacologically close to the wild-type AT_1 receptor (WT) (12). A model based on the early projection map of rhodopsin (47) suggested that the interaction between N111 and N295 stabilizes the AT_1 receptor in the inactive state, and that replacements (as in the N295S mutant) allow the receptor to assume the active state (35). However, data on the constitutive activity of N295S were not confirmed by other studies (12). The model proposed more recently on the basis of the X-ray structure of rhodopsin (46) differs from others by considering direct interactions of the AT_1 receptor with the IC heterotrimeric G protein (40,42). According to this model, the side chain of R126 moves in the activated state from the protonated side chains of D125 and D74 toward *Asp*337 in the Gα chain of the G protein.

The CAMs of the AT_1 receptor contain single and multiple amino acid substitutions of residues F77, L78, S107, F110, N111, L112, L118, M142, L143, P162, E173, I193, L195, T198, I245, W253, N295, and L305 [the numbering of residues based on the rat AT_{1a} receptor sequence, the AT_1 receptors for most species being highly homologous (48)]. Out of these, CAMs with mutations of N111 have been most thoroughly studied, because this mutation provides the highest level of basal activity observed so far for AT_1 CAMs (see, for example, Ref. 29). Extensive systematic studies on single mutations of N111 revealed a clear relation between the size of the residue that replaces N111 and the constitutive activity of the resulting mutants (12,28). Namely, replacements with the smallest residues, Gly and Ala, yielded CAMs with the most pronounced constitutive activity, whereas mutations with bulkier residues yielded less active CAMs. Specifically, the order of basal activity for 10 AT_1 mutants was: N111G > N111S > N111A, N111C > N111I, N111Q, N111H, N111K, N111F, N111Y, the latter mutants showing the same level of basal activity as the WT receptor (12).

The present study employed molecular modeling to reveal conformational changes occurring in the TM region of the AT_1 receptor as a result of mutations of N111 in order to probe possible molecular mechanisms of its constitutive activity. As CAMs do not require binding of an external ligand to be activated, conformational changes in the extracellular domain of AT_1 (the N-terminal tail and the extracellular loops, which are involved in ligand interaction) are less likely to have an important role in the induction of constitutive activity. On the contrary, conformational changes in the TM region could significantly influence the spatial positions of the IC loops and the C-terminal tail, which directly interact with IC-G proteins (4,17,25,30,34,49). The conclusions suggested by the results of molecular modeling obtained in the present study were confirmed with site-directed mutagenesis performed for the suggested double mutants of the AT_1 receptor.

Methods

Molecular modeling

Energy calculations

All energy calculations were performed using the ECEPP/2 force field with rigid valence geometry (50,51). Only *trans*-conformations of Pro residues were considered, and residues of Arg, Lys, Glu, and Asp were present as charged species. Packing of seven-helical bundles for the three-dimensional (3D) model(s) of TM region of AT_1 and the mutants was performed according to a previously described procedure (52). Packing consisted of minimization of the sum of all intrahelical and interhelical interatomic energies in the multidimensional space of parameters that included the 'global' parameters (those related to movements of individual helices as rigid bodies, namely, translations along the coordinate axes *X*, *Y*, *Z* and rotations around these axes T*x*, T*y*, and T*z*) and the 'local' parameters [the dihedral angles of the side chains for all helices; the starting values of those angles were optimized prior to energy minimization by an algorithm described earlier (53); see also below]. The coordinate system for the global parameters was selected as follows: the long axial *X*-coordinate axis for each TM helix (TM1–TM7) has been directed from the first to the last C^{α}-atom; the *Y*-axis was perpendicular to *X* and went through C^{α}-atom of the 'middle' residue of each helix; and the *Z*-axis was built perpendicular to *X* and *Y* to maintain the right-handed coordinate system. For the AT_1 receptor and its mutants, the above 'reference points' in TM helices were defined as follows (see also below) TM1, M30-V41-I53 (the first, middle and last residue, respectively); TM2, F66-L78-E91; TM3, I103-L112-C121; TM4, L143-W153-A163; TM5, I193-L205-I218; TM6, I242-S252-D263; and TM7, M284-T292-F301.

Optimization of spatial arrangement of side chains

The algorithm utilizes a stepwise grid search and consists of several steps (53). First, the θ_1 dihedral angle chosen from the θ_i-angles ($i = 1 \ldots n$), which possess the initial values of $\boldsymbol{\theta}_1^0$, is rotated with a chosen grid step, normally 30°, from −150 to 180°. All other angles are fixed in their $\boldsymbol{\theta}_i^0$-values. Rotation results in the energy profile where some angle value $\boldsymbol{\theta}_1^{\min}$ corresponds to local energy minimum $\mathbf{E_{min}}(\theta_1)$. Then the θ_1-angle is fixed in the $\boldsymbol{\theta}_1^{\min}$-value, and the procedure is repeated for each θ_i-angle to θ_n; at the end of this run all $\boldsymbol{\theta}_i^0$-values became equal to $\boldsymbol{\theta}_i^{\min}$. The second run starts again from θ_1, and so on, until all $\boldsymbol{\theta}_i^{\min}$ do not change any more, which means that the optimal values of θ_i-angles are achieved. The algorithm has been extensively used for optimizing the starting (prior to energy minimization) and final (after energy minimization) values of the dihedral angles of side chains, χ_I (i.e. $\theta_i = \chi_i$), and has been validated by successful design of many biologically active analogs of peptides (54). As an additional benefit, the algorithm produces the energy profiles along the χ_i-angles in the final point of energy minimization revealing a 'slice' of the multidimensional energy surface for each given χ_i. The algorithm is a path-dependent one, because its results may depend on the choice of the initial $\boldsymbol{\theta}_i^0$-values; however, this limitation is easily compensated by changing the order of the initial $\boldsymbol{\theta}_i^0$-angles. In the specific case of the TM bundle of the AT_1 receptor, two independent pathways were applied to select the order of the rotated side chain angles. First, a 'sequential' pathway started from selecting all χ_1-values of TM1 in sequential order, then moved to selecting all χ_2-angles, then all χ_3-angles, etc. until all side chain angles of TM1 were rotated. Then, the pathway involved the χ_i-angles in TM2, TM3, etc. to TM7, and, if necessary, back to TM1 and so on. A second pathway changed the order of selecting the TM segments; instead of selecting TM1, then TM2, then TM3, etc., TM segments were selected in the 'most perturbing order', i.e. first TM3, then TM7, then TM2, then TM6, then TM5, then TM1, and, finally TM4. This order of TM helices goes from those with the maximal number of interhelical interactions to those with the minimal number [see also Ref. (52)]. All changes in side chain rotamers in different mutants of AT_1 reported below were obtained following either pathway independently, suggesting that they were not simply path-dependent procedural artifacts.

Relaxing 3D structure of TM bundles

The process of relaxation of the TM bundle consisted of repeating the general procedure of energy calculations employing the 3D structures of individual TM helices with the spatial arrangement of side chains resulting from packing, as described above, as the starting points. Each individual TM helix has been subjected to re-optimization of the spatial positions of side chains following by re-minimization of the entire intrahelical energy without limitations on the dihedral angles ϕ and Ψ. After that, TM helices were re-packed into the TM bundle as described above.

Simplified energy calculations in the space of global parameters

The term 'simplified energy calculations' refers to helical packing where energy minimization has been performed

only in the space of global parameters (although the values of the dihedral angles of side chains were still optimized prior to energy minimization). Accordingly, the minimized energy consisted only of the interhelical, but not intrahelical, interatomic interactions.

Biologic studies

Mutagenesis of N11G AT_{1a} receptor cDNA

Mutations were introduced into the sequence of the rat AT_{1a} receptor cDNA subcloned into pcDNA3.1/Amp eukaryotic expression vector, using a QuikChange Site-directed Mutagenesis Kit (Stratagene, La Jolla, CA, USA). Each mutant receptor contained a silent restriction endonuclease recognition site to facilitate the screening of clones. After an initial screening performed by restriction enzymes, all mutations were verified by sequencing.

Cell culture and transfection

The CHO-K1 cells were grown in F12K medium (ATCC) containing 10% fetal bovine serum (ATCC), 100 mg/mL streptomycin and 100 IU/mL penicillin (Invitrogen Inc., Carlsbad, CA, USA). Transient transfections were performed in 24-well plates using Lipofectamine reagent (Invitrogen Inc.) as previously described (55). Cell culture media, transfection reagents, ATCC, and fetal bovine serum were purchased from Invitrogen Inc.

[Sar^1, Ile^8]-angiotensin II binding to receptor mutants

The number of angiotensin II-binding sites was determined by incubating the transfected cells with ^{125}I-[Sar^1, Ile^8]-angiotensin II (Gene Logic, Inc., Gaithersburg, MD, USA) and increasing concentrations of the unlabeled peptide in M-199 medium containing 25 mM HEPES (pH 7.4) for 6 h at 4 °C. The cells were then washed twice with ice-cold phosphate-buffered saline, and their bound radioactivity was determined by γ-spectrometry. The displacement curves were analyzed with the KELL computer program using a one-site model.

Inositol phosphate measurements

Approximately 24 h after transfection, the culture medium was replaced and cells were metabolically labeled overnight in 0.5 mL of inositol-free M-199 containing 1 g/L bovine serum albumin, 2.5% fetal bovine serum, 100 IU/mL penicillin, 100 μg/mL streptomycin and 10–20- μCi/mL *myo*-[2-^{3}H]inositol (Amersham Biosciences, Piscataway, NJ, USA). After labeling, the cells were washed twice with medium M-199 containing 25 mM HEPES (pH 7.4; Biofluids, Rockville, MD, USA), and incubated in the same medium for 30 min at 37 °C in the presence of 10 mM LiCl. Cells were then stimulated with increasing concentrations of angiotensin II, CGP-42112A, or angiotensin IV for 20 min, and reactions were terminated by placing the plates on ice and adding 10 mM ice-cold formic acid. After 30 min on ice, samples were applied directly to columns of AG1-X8 ion exchange chromatography resin (Bio-Rad Laboratories, Inc., Hercules, CA, USA). The columns were washed three times with 1 mL of water to remove free inositol, and inositol monophosphates were collected by washing the columns with 2 × 3 mL of 0.2 M ammonium formate in 10 mM formic acid. The $InsP_2$ + $InsP_3$ fractions were then eluted with 1 M ammonium formate in 10 mM formic acid, and their radioactivities were determined by liquid scintillation.

Evaluation of constitutive activity

Constitutively active GPCRs exhibit elevated basal signaling activity, relative to that of the WT receptor (3), as well as high sensitivity to certain partial agonists and other specific ligands of the WT receptor. Constitutively active AT_1 receptors are sensitive to partial agonists such as CGP-42112A, a peptide agonist for the angiotensin AT_2 receptor with the sequence *N*-α-nicotinoyl-Tyr-(*N*-α-CBZ-Arg)-Lys-His-Pro-Ile-OH (13), as well as [Sar^1, Ile^4, Ile^8]-angiotensin II, a weak AT_1 receptor antagonist (28) and angiotensins 3–8 (angiotensin IV), another weak AT_1 receptor antagonist that is a full and potent agonist for the N111G AT_1 receptors (33). In the present study, both CGP-42112A and angiotensin IV were used to evaluate the properties of double mutants of the constitutively active AT_1 receptor.

Results

Three mutants of the AT_1 receptor, namely N111G, N111A, and N111W, as well as WT, were selected for molecular modeling. The first two mutants, N111G and N111A, are well known as the most activated AT_1 CAMs obtained by single mutations (12,15), whereas N111W was expected to be as silent as WT because the mutants N111F, N111Q or N111I are silent (12) in the absence of an agonist, and the size of the Trp side chain is larger than those of residues Phe, Gln or Ile [this suggestion has been confirmed in a study in which N111W was shown to possess the same low basal activity as WT (56)]. Accordingly, we sought conformational differences that might occur in the TM

regions of the pronounced CAMs, N111G, and N111A, compared with the silent WT and N111W receptors.

Unrelaxed 3D models of the TM regions of WT and the mutants

Most methods employed in building 3D model(s) of the TM region of the AT_1 receptor and its mutants were essentially the same as described earlier for bacteriorhodopsin (57) and rhodopsin (58). First, the sequence of the rat AT_1 receptor has been aligned to that of bovine rhodopsin by the CLUSTAL w procedure available at the Internet http://ca.expasy.org/tools. The alignment is shown in Table 1; it is quite satisfactory, as positions that are occupied by the conservative residues according to the multisequence alignment over the entire rhodopsin family of GPCRs (59; expressed in bold in Table 1) are almost invariably (32 of 36 cases) occupied by the same or homologous residues in the aligned AT_1 sequence, the exceptions being D74 (instead of the conservative residue L), C76 (L), D237 (K), and N295 (S). The end points of TM helices were found by the nonstatistical procedure developed earlier (60); TM helical segments TM1–TM7 are underlined in Table 1.

Then, the low-energy conformations for each individual TM helical segment were found by energy minimization starting from the all-helical backbone conformations (i.e. the values of all dihedral angles ϕ and Ψ were initially of $-60°$). Some limitations on the ϕ- and Ψ-values ($-30° \geq \phi$, $\Psi \geq -90°$) were placed during energy minimization to mimic, to some extent, limitations on intrahelical mobility of TM segments immobilized in the membrane. The 'global' starting point for assembling the TM bundle for AT_1 and its mutants was the X-ray structure of dark-adapted rhodopsin (46). At the stage of helical packing, the dihedral angles ϕ and Ψ were 'frozen' at the values previously obtained by energy minimization of the individual helices (hence, the term 'unrelaxed' models).

The resulting 3D model of the TM region of the AT_1 receptor differed from the corresponding region of rhodopsin by the rms value of 2.77–2.83 Å (here and throughout the text, the rms values were calculated for C^{α}-atoms only) depending on the order of optimizing of the side chains (see above). The 3D models of WT and the mutants were quite similar, with rms values of the mutants compared with AT_1 being approximately 0.3–0.6 Å. The energetic patterns of interhelical interactions were also similar: aside from

Table 1. **Sequence of the bovine Rh (the upper line) aligned to sequence of the rat AT_1 receptor (the lower line).**

```
  MNGTEGPNFYVPFSNKTGVVRSPFEAPQYYLAEPWQFSMLAAYMFLLIMLGFPINFLTL
  --------MALNSSAEDGIKRIQDDCPKAGRHS-YIFVMIPTLYSIIFVVGIFGNSLVV
          |        |         |          |         |         |
          1        10        20         30        40        50

YVTVQHKKLRTPLNYILLNLAVADLFMVFGGFTTTLYTSLHGYFVFGPTGCNLEGFFATL
IVIYFYMKLKTVASVFLLNLALADLCFLLTLPLWAVYTAMEYRWPFGNHLCKIASASVSF
          |        |         |          |         |         |
         60        70        80         90       100       110

GGEIALWSLVVLAIERYVVVCKPMSN-FRFGENHAIMGVAFTWVMALACAAPPLVGWSRY
NLYASVFLLTCLSIDRYLAIVHPMKSRLRRTMLVAKVTCIIIWLMAGLASLPAVIHRNVY
          |        |         |          |         |         |
        120       130       140        150       160       170

IPEGMQCSCGIDYYTPHEETNNESFVIYMFVVHFIIPLIVIFFCYGQLVFTVKEAAAQQQ
FIENTNITVCAFHYESRNSTLPIGLGLTKNILGFLFPFLIILTSYTLIWKALKKAYEIQK
          |        |         |          |         |         |
        180       190       200        210       220       230

ESATTQKAEKEVTRMVIIMVIAFLICWLPYAGVAFY--------IFTHQGSDFGPIFMTIPAFF
N----KPRNDDIFRIIMAIVLFFFFSWVPHQIFTFLDVLIQLGVIHDCKISDIVDTAMPITICI
             |         |         |         |         |         |
           240       250       260       270       280       290

AKTSAVYNPVIYIMMNKQFRNCMVTTLCCG------KNPLGDDEASTTVSKTETSQVAPA
AYFNNCLNPLFYGFLGKKFKKYFLQLLKYIPPKAKSHSSLSTKMSTLSYRPSDNMSSSAK
          |        |         |         |         |         |
        300       310       320       330       340       350

--------- 348
KPASCFEVE 359
```

Numbering is according to the angiotensin receptor type 1 (AT_1) sequence. transmembrane helical segments determined for the AT_1 are underlined. Residues found as highly conservative in multi-sequence alignment over the entire rhodopsin-like family of G protein-coupled receptor are shown in bold letters.

interactions between the neighboring helices, the most significant interactions were between helices TM2 and TM7, TM2 and TM4, TM2 and TM6, and TM3 and TM6 in all cases. The least significant interactions were between helices TM1 and TM3, TM1 and TM5, and TM5 and TM7. The differences, however, occurred in intrahelical interactions within TM4; namely, energies of these interactions relative to the energy in WT were approximately 91 kcal/mol for N111G and approximately 90 kcal/mol for N111A, but not for N111W where the energy was basically the same as in WT. In other words, the unrelaxed 3D models of the TM helical bundles reveal significant steric hindrance in TM4 in the more pronounced CAMs (N111G and N111A), but not in the non-CAMs N111W and WT; possible reasons for these differences are discussed below.

Individual rotations of TM helices do not distinguish CAMs from non-CAMs

The most likely conformational transitions occurring during transfer from the ground to activated state in the TM region of rhodopsin, the only GPCR with a known X-ray structure of the dark-adapted state (46,61–64), are rotations around the long T*x*-axes and simultaneous transitional movements of helices TM6, and, to the less extent, TM3, as rigid bodies. These suggestions were based on experimental observation made mostly by site-directed spin labeling (see the reviews 65–67), and are consistent with our results of molecular modeling of the photoactivated state of rhodopsin (58). Concerted rotations and/or movements of some TM helices have also been suggested as the main conformational changes distinguishing the active from the inactive state in the β_2-adrenergic receptor (68–71), the α-adrenergic receptor (72), and other GPCRs (73,74), etc., including the AT_1 receptor (31). To explore this possibility, independent rotations around the T*x*-axis on a grid of 30° were considered for each TM helix, starting from the initial rhodopsin-like 3D models of the TM bundle of WT and the mutants N111G, N111A, and N111W. 12 positions of the T*x*-values were considered for each TM helix; all other starting values for global parameters were the same as in the initial models of the corresponding TM bundles. Simplified energy calculations performed for each position of T*x*'s yielded energetic profiles for each helix; basically, the same procedure was applied earlier for rhodopsin (58).

The results obtained, however, in contrast to those for photoactivated rhodopsin, did not allow selection of any specific set of T*x*-values that would correspond to the low-energy conformations of the TM regions for mutants N111G and N111A (CAMs), on the one hand, vs. WT and N111W (non-CAMs) on the other (data not shown). The largest differences in exact positions of local energy minima for CAMs and non-CAMs were only approximately 30° for TM3, TM4, and TM5 [compare with TM6 in rhodopsin, where the difference between T*x*-values in the dark-adapted and activated states was approximately 120° (58)]. On the contrary, combinations of the T*x*-values roughly corresponding to the initial rhodopsin-like 3D models of the TM bundles were the only low-energy conformers shared by both CAMs and non-CAMs.

Spatial positions of several side chains are different in CAMs and non-CAMs

A clear distinction in the pattern of low-energy spatial positions of several side chains was observed between WT on the one hand, and N111G and N111A, on the other. The most pronounced differences between WT and N111G are listed in Table 2. The same differences occurred between WT and N111A; no significant differences in side chain orientations were detected between WT and N111W.

More detailed evaluation of the above differences and their energetic consequences is consistent with the following possible pathway of conformational changes that lead to constitutive activity of N111G and N111A (Fig. 1). Namely, there are two local 'microdomains' (the term from Ref. 75) in the WT receptor. The first is formed due to favorable interactions of the side chains of N111, N295, and F77, and the second is formed between the side chains of L112, Q257, and Y113. The side chain of L112 possesses

Table 2. **Differences in low-energy spatial positions of side chains between wild type (WT) and N111G**

Residue	Angle	WT	N111G
F77	χ_1	−150 and 150	150
L112	χ_1	From −120 to 150	From −90 to 120
Y113	χ_1	From −90 to −120	From −150 to 180
F117	χ_1	−60	From −120 to −150
I152	χ_1	−80	70
	χ_2	From 150 to 180	From 90 to 120
M155	χ_2	From −60 to 180	From −60 to −120
Q257	χ_1	−150	From −150 to 150
N295	χ_1	From −90 to −120	From −90 to −150

The approximate values (or ranges defined by energetic profiles) for dihedral angles are listed in degrees.

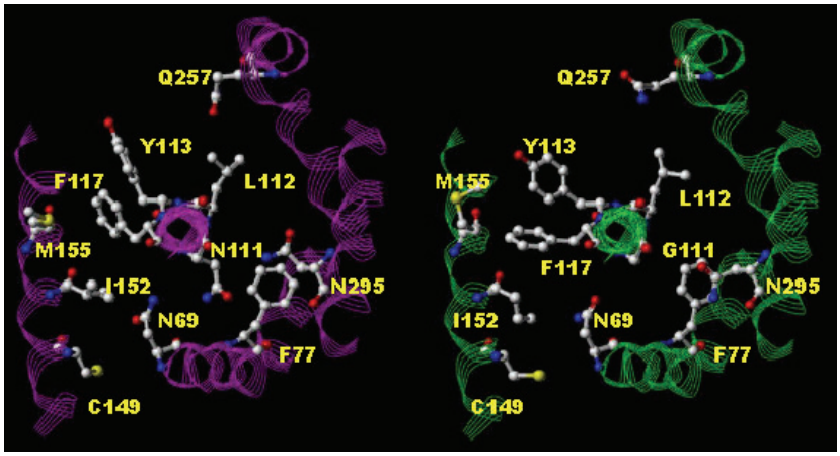

Figure 1. Conformational changes from wild type (WT; left) to N111G (right). Only residues mentioned in text are shown. All hydrogens are omitted for clarity. TM2, TM3, TM4, TM6, and TM7 are shown as line ribbons (magenta in WT, green in N111G). The view is from the intracellular side of the membrane along the T*x*-axis of TM3.

significant mobility (see Table 2), which ensures dynamic equilibrium between the two microdomains. When N111 is mutated to glycine (see Fig. 1), the first microdomain loses the important N111–N295 and N111–F77 interactions, so the side chains of F77 and N295 move closer to each other to preserve their favorable interactions. This opens a cavity for the side chain of L112 to move toward F77 and N295. As a consequence, favorable interactions L112–Q257 and L112–Y113 are disrupted, and it becomes energetically more favorable for the side chain of Y113 to move toward F117. In turn, the side chain of F117 changes the spatial orientation and clashes with side chains of I152 and M155 in TM4. The side chain of M155 relieves this potential steric hindrance by changing the value of the χ_2-angle (see Table 2); however, the side chain of I152, despite any possible changes in the χ_1/χ_2-values, is trapped in the closed hindered pocket formed by F111, C149, and N69. Obviously, the described changes do not occur sequentially as described as step-by-step, but in a dynamic equilibrium between the resting and activated states (compare two panels in Fig. 1).

Relaxing steric hindrance in 3D models of activated states

Possible ways to avoid the significant steric hindrance in the I152–C149–N69–F117 pocket and relax the structure require either changing the values of the backbone dihedral angles in TM4, or movement of TM4 relative to other TM helices, or both. Relaxation of the calculated structures was performed as described in the Methods section for WT and for the mutants N111G and N111W, and yielded three main observations. First, the backbone structure of all individual TM helices including TM4 remained practically the same as in the unrelaxed structures of the WT and mutant receptors (the rms values between relaxed and unrelaxed helices ranged from 0.2 to 0.6 Å). However, the overall difference between the relaxed TM bundles of WT and N111G was somewhat higher than between the unrelaxed models (rms value of 1.7 Å compared with approximately 0.5 Å, see above). Secondly, the characteristic patterns of the conformational changes in the side chains described above for the unrelaxed structures of WT, N111G (Table 2) and N111W did not change in the relaxed structures. Thirdly, TM4 helix in N111G moved as a rigid body somewhat outside the core of the structure and toward the extracellular part of the membrane for about a half of a helical turn (see Fig. 2); this movement was not observed in WT and N111W. It is possible that this particular movement would significantly change the potential conformations of IC loop (IC2) that connects TM3 and TM4, a known interaction site with G proteins.

Discussion

The molecular mechanism of constitutive activity in mutant AT_1 receptors suggested by molecular modeling needs validation from available experimental data. Unfortunately, direct structural data describing the activated state(s) of the AT_1 receptor, including the 3D structure(s) of CAMs, are practically absent, except for estimations of the accessibility of cysteines to sulfhydryl-reacting reagents in Cys-containing mutants of AT_1 in either the WT or N111G genetic backgrounds (31,32,36,37). Structural interpretation of such effects is rather complicated (e.g. see discussion in Ref. 58), and studies performed by two different groups (31,32,36) yield somewhat different conclusions. Differences in the accessibilities of cysteines in the mutants containing cysteines in TM2 have been interpreted as indications of global movement of TM2 (31) involving changes in interactions between TM2 and TM7 (32), whereas according to Ref. (36) the results of the Cys-scan along TM7 suggest

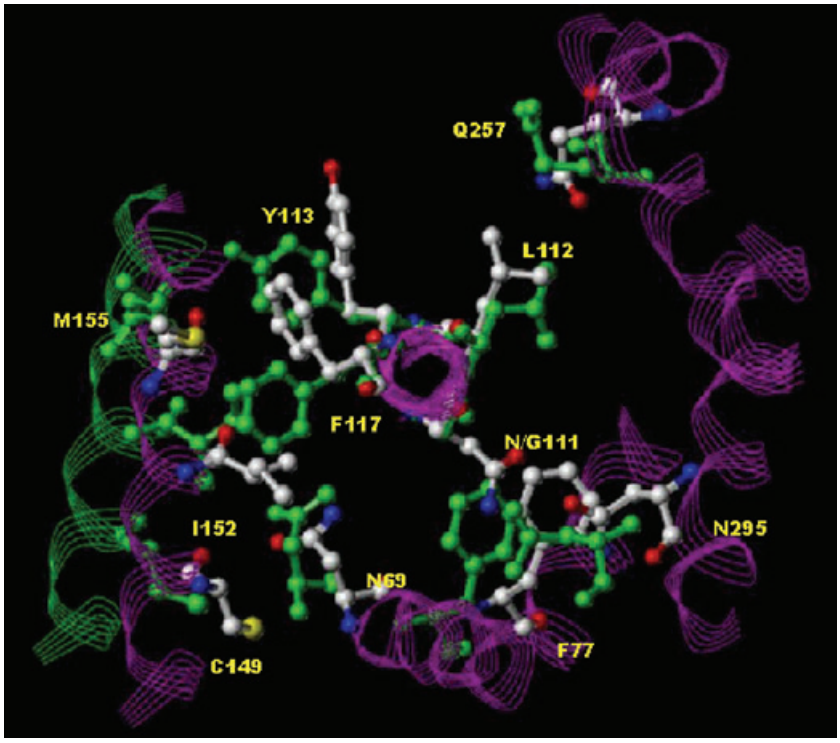

Figure 2. Relaxed structures of wild type (WT; generic atom colors) and N111G (green) overlapped over TM3. Only residues mentioned in text are shown. All hydrogens are omitted for clarity. TM2, TM3, TM4, TM6, and TM7 in WT are shown as line ribbons in magenta; TM4 in N111G is shown as line ribbon in green. Note the translational shift in positions of TM4 helices (lower left corner). The view is from the intracellular side of the membrane along the T*x*-axis of TM3.

movement of this helix. Later, the same group suggested also slight (by 45°) rotation of TM3 (37). Notably, in all cases the suggested movements were of small magnitude.

One confirmation for the predicted mechanism of constitutive activation comes from studies on mutations of L112. As was described above, the bulky side chain of L112 plays an extremely important role in maintaining a delicate balance of interactions within the two microdomains described above, namely N111–N295–F77 and L112–N257–Y113, as well as between them. Energy calculations showed that L112F, a mutant with replacement of L112 for a bulkier residue, possesses the characteristic pattern of conformational changes in the side chains of L112, Y113, F117, I152, and M155 suggested above for N111G and N111A; this pattern is absent in L112C, a mutant with replacement of L112 for a smaller residue. Also, the diagnostic steric hindrance found in TM4 for the unrelaxed 3D models of N111G and N111A is present in L112F, but not L112C (in the nonrelaxed 3D models; in the relaxed 3D model of L112F the hindrance is eliminated, but the pattern of conformational changes remains the same as in N111G). These results led to the prediction that L112F should display constitutive activity, and L112C should be a silent mutant. Indeed, the double mutant V164A/L112F has been described in the literature as possessing high affinity for AT_1 receptor ligands and showing constitutive activity slightly above of that of WT; mutants with the L112H substitution showed even higher levels of constitutive activity (29). It is noteworthy that those mutants do not possess replacements of N111 for glycine or alanine. On the contrary, the L112C mutant is silent [E. Escher, personal communication; see also Ref. (37)]. In the same line, the chimeric receptor CR18 that involves mutation of L112 to a bulkier Met residue is also a CAM (12).

The proposed molecular mechanism of constitutive activity in the AT_1 receptors may not coincide with the mechanism of activation by its endogenous ligand, angiotensin II (Asp^1-Arg^2-Val^3-Tyr^4-Ile/Val^5-His^6-Pro^7-Phe^8). However, the unrelaxed 3D model of the complex of the TM region of the AT_1 receptor and angiotensin II proposed by us earlier (57) contains the same conformational pattern of the side chain arrangements for Y113, F117, and I152 with the same steric hindrance in TM4. The complex is depicted in Fig. 3 in the same projection as the 3D model in Fig. 2. One can clearly see the conformational changes in question; however, in this case, interactions within the microdomains N111–N295–F77 and L112–Q257–Y113 are changed not by spontaneous movement of the side chain of L112 toward F77 and N295, but by interactions with the C-terminal part of angiotensin II, which completely disrupts interaction Q257–L112 and pushes L112 toward Y113. Then, the same cascade of conformational changes as in N111G is initiated, including placing of the side chain of I152 into the closed hindered pocket formed by F111, C149, and N69 (see Fig. 3). As the present study and that of the 3D model of the complex of the TM region of the AT_1 receptor

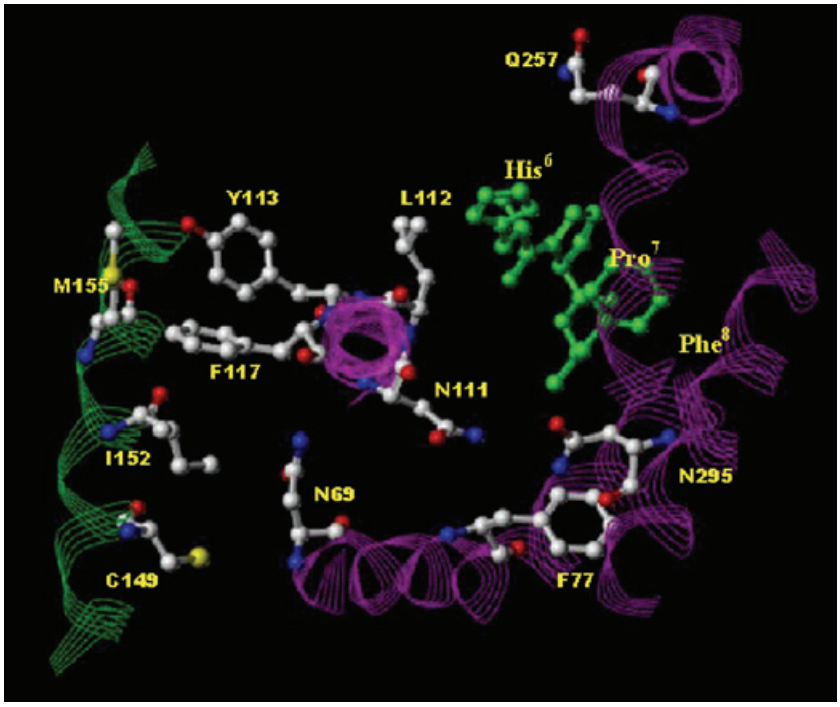

Figure 3. Conformational changes occurring in the complex angiotensin type 1 (AT_1)–angiotensin II. For AT_1, only residues mentioned in text are shown (generic atom colors). For angiotensin II, only residues His^6, Pro^7, and Phe^8 (in green) directly interacting with N111 and L112 are shown. All hydrogens are omitted for clarity. TM2, TM3, TM6, and TM7 are shown as line ribbons in magenta, TM4 is shown as line ribbon in green. The view is from the intracellular side of the membrane along the T*x*-axis of TM3.

and angiotensin II (57) were completely independent, the similar conformational changes found in both studies may, in our view, complement each other and strengthen the proposed model for constitutive activity.

The proposed hypothesis of characteristic conformational changes in the CAMs with mutations of N111 was verified by making double mutants of the AT_1 receptor that contain the constitutively active mutation N111G together with additional replacement of the residues involved in the above changes, L112, Y113, F117, and I152, by Ala. Such additional mutations will replace the sizable side chains by much less voluminous alanine residues, but presumably will not influence the general helical backbone structure of TM3 or TM4. Energy calculations performed for the double mutants N111G/L112A, N111G/Y113, N111G/F117, and N111G/I152A (the unrelaxed models) showed that the former mutant retained the pattern of side chain rotations characteristic for N111G and N111A, as well as some steric hindrance in TM4 (although smaller than in N111G or N111A) and, therefore, might display constitutive activity. In the other three double mutants, the pattern in question is interrupted, and there is no steric hindrance in TM4; therefore, such mutants are expected to exhibit less constitutive activity than N111G, if any.

Generally, these predictions were confirmed by experimental studies. Five mutants, namely N111G, N111G/L112A, N111G/Y113, N111G/F117, and N111G/I152A were obtained by site-directed mutagenesis in COS-7 cells as described in Methods. The mutants were characterized by binding studies with ^{125}I-angiotensin and by stimulation with angiotensin II as well as the angiotensins 3–8 hexapeptide (angiotensin IV) and CGP-42112A (Fig. 4A,B; data related to CGP-42112A not shown). The N111G/Y113 mutant was poorly expressed (approximately 5% compared

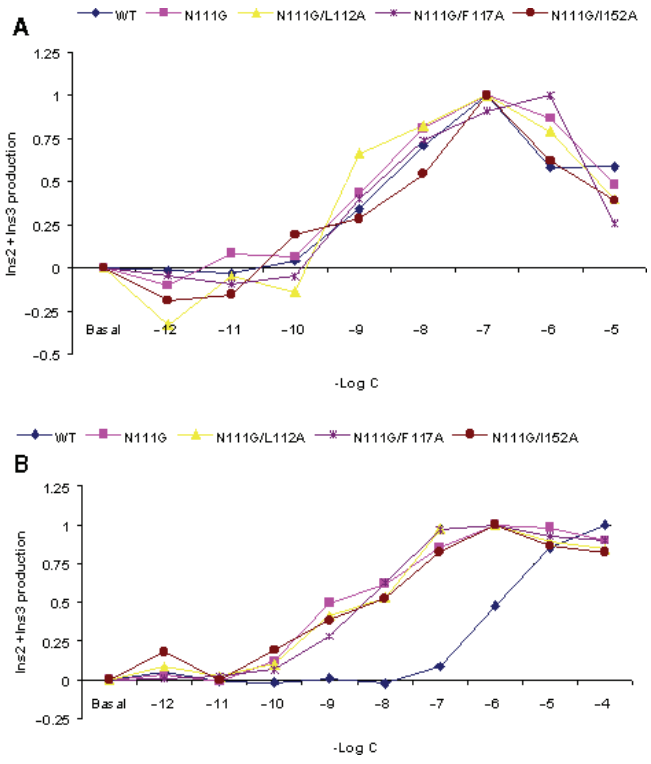

Figure 4. Stimulation of receptors by angiotensin (A) and angiotensin IV (B). The data are normalized to the maximal level of inositol phosphate (IP) production for each receptor.

with WT); therefore, the data related to this mutant cannot be reliably interpreted. The basal levels of $InsP_2 + InsP_3$ production were 2.4 ± 0.4; 2.1 ± 0.3; 1.0 ± 0.1 and 2.6 ± 0.3 for N111G, N111G/L112A, N111G/F117 and N111G/I152A, respectively (relative to 1.0 for WT). Stimulating the mutants with angiotensins 3–8 (Fig. 4B) clearly demonstrated the ability of the mutants in question to display constitutive activity. Similar dependences were obtained by stimulation by CGP-42112A (data not shown). Both peptides caused significant increases in $InsP_{2+3}$ levels in cells transfected with the N111G AT_1 CAMs, but had negligible effects on the WT receptor (e.g. see Fig. 4B).

These findings indicate that the proposed molecular mechanism for constitutive activity of the AT_1 receptor mutants correctly predicted the constitutive activity of the double mutants N111G/L112A and N111G/F117A. The basal activity of N111G/I152A was somewhat higher than expected, and that of N111G/Y113A was difficult to estimate due to poor expression of the mutant.

It should be emphasized that the proposed molecular mechanism for conformational changes leading to constitutive activity in the mutants of the AT_1 receptor may be the major one, but need not be unique. For instance, energy calculations performed for the double mutant F77Y/W253R, which displays some constitutive activity (29), showed neither the characteristic pattern of conformational changes, nor steric hindrance in TM4 (the unrelaxed model). Also, a variety of other CAMs described in the literature [mostly in Ref. (29)] possess mutations in the IC loops or the C-terminal tail of the AT_1 receptor, which may directly interact with G proteins (for instance, L305Q). Obviously, conformational changes associated with such mutations may be quite different from those proposed in the present study.

Concluding Remarks

The present study describes a possible molecular mechanism for constitutive activity of double mutants of the N111G AT_1 receptor. It was proposed that the mechanism involves a cascade of conformational changes in spatial positions of side chains along TM3 from L112 to Y113 to F117, which in turn, results in conformational changes in TM4 (I152 and M155) leading to the movement of TM4 as a whole. As a consequence, the position of the IC loop interacting with the G protein is perturbed. This mechanism is supported by correct predictions of the constitutive activity of mutants L112F and L112C, as well as of the double mutants N111G/L112A and N111G/F117A. The basal activity of N111G/I152A was somewhat higher than expected, and that of N111G/Y113A was not estimated due to poor expression of the mutant.

The current general view on the molecular mechanism of constitutive activation is that one has to abolish specific constraining intramolecular interactions existing in a resting state of the silent receptors to gain constitutive activity (3). Our study suggests a more complicated mechanism: when specific intramolecular interactions (such as those involving the N111 side chain) are abolished, this initiates conformational changes that introduce some other constraints (steric hindrance) in the other parts of the molecule. In turn, releasing those constraints becomes a driving force for activation of the AT_1 receptor. As regards, the proposed mechanism of constitutive activity of the AT_1 receptor reveals a somewhat novel view on the problem, because it clearly demonstrates complexity of the process of receptor activation. The mechanism also differs from the proposed mechanism of activation of rhodopsin (58).

The results of the present study may also have more general impact on our efforts to understand conformational changes occurring during activation of GPCRs [see also a recent review from Ref. (76)]. While it is tempting to propose a general model for activation of all GPCRs based either on the role of helical movements (rotations, tilts and/or kinks) [see, for example, Ref. (1)], or on the role of conformational changes in the conserved side chains [see Ref. (75)], a more general approach to model the activated states of different GPCRs is recommended. The approach developed in this and earlier studies (58) employs, as the first step, integrated modeling of the TM bundles of GPCRs that regards both movements of TM helices as rigid bodies and the concerted rotations of the individual side chains as equally important factors leading to activation of GPCRs. Therefore, our approach automatically accounts for the fact that different factors may have different significance in different GPCRs. The next logical step would be to restore possible conformations of the non-TM parts of the AT_1 receptor, such as the N- and C-terminal tails and the interhelical loops, followed by modeling of conformational changes in receptors caused by ligand binding; the corresponding modeling tools are already developed and are available [see, for example, Ref. (52,57,77)].

Acknowledgements: The authors are grateful to Dr Emanuel Escher (University of Sherbrook, Sherbrook, Canada) for providing information on constitutive activity of the L112C mutant. Drs Emanuel Escher and Tom Baranski (Washington University, St Louis, MO) are also acknowledged for helpful discussions and comments on the manuscript. This work was supported by NIH grant GM 53630.

References

1. Gether, U. (2000) Uncovering molecular mechanisms involved in activation of G protein-coupled receptors. *Endocr. Rev.* **21**, 90–113.
2. Drews, J. (2000) Drug discovery: a historical perspective. *Science* **287**, 1960–1964.
3. Parnot, C., Miserey-Lenkei, S., Bardin, S., Corvol, P. & Clauser, E. (2002) Lessons from constitutively active mutants of G protein-coupled receptors. *Trends Endocrinol. Metab.* **13**, 336–343.
4. Shibata, T., Suzuki, C., Ohnishi, J., Murakami, K. & Miyazaki, H. (1996) Identification of regions in the human angiotensin II receptor type 1 responsible for Gi and Gq coupling by mutagenesis study. *Biochem. Biophys. Res. Commun.* **218**, 383–389.
5. Schambye, H.T., Hjorth, S.A., Bergsma, D.J., Sathe, G. & Schwartz, T.W. (1994) Differentiation between binding sites for angiotensin II and nonpeptide antagonists on the angiotensin II type 1 receptors. *Proc. Natl Acad. Sci. U S A* **91**, 7046–7050.
6. Schambye, H.T., Vonwijk, B., Hjorth, S.A., Wienen, W., Entzeroth, M., Bergsma, D.J. & Schwartz, T.W. (1994) Mutations in transmembrane segment VII of the AT_1 receptor differentiate between closely related insurmountable and competitive angiotensin antagonists. *Br. J. Pharmacol.* **113**, 331–333.
7. Hjorth, S.A., Schambye, H.T., Greenlee, W.J. & Schwartz, T.W. (1994) Identification of peptide binding residues in the extracellular domains of the AT_1 receptor. *J. Biol. Chem.* **269**, 30953–30959.
8. Hunyady, L., Balla, T. & Catt, K.J. (1996) The ligand binding site of the angiotensin AT_1 receptor [review]. *Trends Pharmacol. Sci.* **17**, 135–140.
9. Hunyady, L., Ji, H., Jagadeesh, G., Zhang, M., Gaborik, Z., Mihalik, B. & Catt, K.J. (1998) Dependence of AT_1 angiotensin receptor function on adjacent asparagine residues in the seventh transmembrane helix. *Mol. Pharmacol.* **54**, 427–434.
10. Yamano, Y., Ohyama, K., Kikyo, M., Sano, T., Nakagomi, Y., Inoue, Y., Nakamura, N., Morishima, I., Guo, D.F., Hamakubo, T. & Inagami, T. (1995) Mutagenesis and the molecular modeling of the rat angiotensin II receptor AT_1. *J. Biol. Chem.* **270**, 14024–14030.
11. Feng, Y.H., Noda, K., Saad, Y., Liu, X.P., Husain, A. & Karnik, S.S. (1995) The docking of Arg^2 of angiotensin II with Asp^{281} of AT_1 receptor is essential for full agonism. *J. Biol. Chem.* **270**, 12846–12850.
12. Feng, Y.-H., Miura, S., Husain, A. & Karnik, S.S. (1998) Mechanism of constitutive activation of the AT_1 receptor: influence of the size of the agonist switch binding residue asn^{111}. *Biochemistry* **37**, 15791–15798.
13. Monnot, C., Bihoreau, C., Conchon, S., Curnow, K.M., Corvol, P. & Clauser, E. (1996) Polar residues in the transmembrane domains of the type 1 angiotensin II receptor are required for binding and coupling – reconstitution of the binding site by co-expression of two deficient mutants. *J. Biol. Chem.* **271**, 1507–1513.
14. Groblewski, T., Maigret, B., Nouet, S., Larguier, C., Bonnafous, J.-C. & Marie, J. (1995) Amino acids of the third transmembrane domain of the AT_{1a} angiotensin ii receptor are involved in the differential recognition of peptide and nonpeptide ligands. *Biochem. Biophys. Res. Commun.* **209**, 153–160.
15. Groblewski, T., Maigret, B., Larguier, R., Lombard, C., Bonnafous, J.-C. & Marie, J. (1997) Mutation of Asn^{111} in the third transmembrane domain of the AT_{1a} angiotensin ii receptor induces its constitutive activation. *J. Biol. Chem.* **272**, 1822–1826.
16. Bihoreau, C., Monnot, C., Davies, E., Teutsch, B., Bernstein, K.E., Corvol, P. & Clauser, E. (1993) Mutation of Asp^{74} of the rat angiotensin-II receptor confers changes in antagonist affinities and abolishes G-protein coupling. *Proc. Natl Acad. Sci. U S A* **90**, 5133–5137.
17. Conchon, S., Barrault, M.-B., Miewrey, S., Corvol, P. & Clauser, E. (1997) The C-terminal third intracellular loop of the rat AT_{1a} angiotensin receptor plays a key role in G protein coupling specificity and transduction of the mitogenic signal. *J. Biol. Chem.* **272**, 25566–25572.
18. Costa-Neto, C.M., Mikakawa, A.A., Oliveira, L., Hjorth, S.A., Schwartz, T.W. & Paiva, A.C.M. (2000) Mutational analysis of the interaction of the N- and C-terminal ends of angiotensin II with the rat AT_{1a} receptor. *Br. J. Pharmacol.* **130**, 1263–1268.
19. Costa-Neto, C.M., Mikakawa, A.A., Pesquero, J.B., Oliveira, L., Hjorth, S.A., Schwartz, T.W. & Paiva, A.C.M. (2002) Interaction of a non-peptide agonist with angiotensin II AT_1 receptor mutants. *Can. J. Physiol. Pharmacol.* **80**, 413–417.
20. Han, H., Shimuta, S.I., Kanashiro, C.A., Oliveira, L., Han, S.W. & Paiva, A.C.M. (1998) Residues Val^{254}, His^{256}, and Phe^{259} of the angiotensin II AT_1 receptor are not involved in ligand binding but participate in signal transduction. *Mol. Endocrinol.* **12**, 810–814.
21. Inoue, Y., Nakamura, N. & Inagami, T. (1997) A review of mutagenesis studies of angiotensin II type 1 receptor, the three-dimensional receptor model in search of the agonist and antagonist binding site and the hypothesis of a receptor activation mechanism [review]. *J. Hypertens* **15**, 703–714.
22. Ji, H., Leung, M., Zhang, Y., Catt, K.J. & Sandberg, K. (1994) Differential structural requirements for specific binding of nonpeptide and peptide antagonists to the at_1 angiotensin receptor. *J. Biol. Chem.* **269**, 16533–16536.
23. Marie, J., Maigret, B., Joseph, M.P., Larguier, R., Nouet, S., Lombard, C. & Bonnafous, J.C. (1994) Tyr^{292} in the seventh transmembrane domain of the AT_{1a} angiotensin II receptor is essential for its coupling to phospholipase C. *J. Biol. Chem.* **269**, 20815–20818.
24. Miura, S., Feng, Y.H., Husain, A. & Karnik, S.S. (1999) Role of aromaticity of agonist switches of angiotensin II in the activation of the AT_1 receptor. *J. Biol. Chem.* **274**, 7103–7110.
25. Miura, S., Zhang, J. & Karnik, S.S. (2000) Angiotensin II type 1 receptor-function affected by mutations in cytoplasmic loop CD. *FEBS Lett.* **470**, 331–335.
26. Noda, K., Saad, Y., Kinoshita, A., Boyle, T.P., Graham, R.M., Husain, A. & Karnik, S.S. (1995) Tetrazole and carboxylate groups of angiotensin receptor antagonists bind to the same subsite by different mechanisms. *J. Biol. Chem.* **270**, 2284–2289.
27. Noda, K., Saad, Y. & Karnik, S.S. (1995) Interaction of Phe^8 of angiotensin II with Lys^{199} and His^{256} of AT_1 receptor in agonist activation. *J. Biol. Chem.* **270**, 28511–28514.
28. Noda, K., Feng, Y.H., Liu, X.P., Saad, Y., Husain, A. & Karnik, S.S. (1996) The active state of the AT_1 angiotensin receptor is generated by angiotensin II induction. *Biochemistry* **35**, 16435–16442.

29. Parnot, C., Bardin, S., Miserey-Lenkei, S., Guedin, D., Corvol, P. & Clauser, E. (2000) Systematic identification of mutations that constitutively activate the angiotensin II type 1a receptor by screening a randomly mutated cDNA library with an original pharmacological bioassays. *Proc. Natl Acad. Sci. U S A* **97**, 7615–7620.
30. Tang, H., Guo, D.F., Porter, J.P., Wanaka, Y. & Inagami, T. (1998) Role of cytoplasmic tail of the type 1a angiotensin II receptor in agonist- and phorbol ester-induced desensitization. *Circ. Res.* **82**, 523–531.
31. Miura, S. & Karnik, S.S. (2002) Constitutive activation of angiotensin II type 1 receptor alters the orientation of transmembrane helix-2. *J. Biol. Chem.* **277**, 24299–24305.
32. Miura, S., Zhang, J., Boros, J. & Karnik, S.S. (2003) TM2-TM7 interaction in coupling movement of transmembrane helices to activation of the angiotensin II type-1 receptor. *J. Biol. Chem.* **278**, 3720–3725.
33. Le, M.T., Vanderheyden, P.M.L., Szaszak, M., Hunyady, L. & Vauquelin, G. (2002) Angiotensin IV is a potent agonist for constitutive active human AT_1 receptors. *J. Biol. Chem.* **277**, 23107–23110.
34. Zhang, M., Zhao, X., Chen, H.-C., Catt, K.J. & Hunyady, L. (2000) Activation of the AT_1 angiotensin receptor is dependent on adjacent apolar residues in the carboxyl terminus of the third cytoplasmic loop. *J. Biol. Chem.* **275**, 15782–15788.
35. Balmforth, A.J., Lee, A.J., Warburton, P., Donnelly, D. & Ball, S.G. (1997) The conformational change responsible for AT_1 receptor activation is dependent upon two juxtaposed asparagine residues on transmembrane helices III and VII*. *J. Biol. Chem.* **272**, 4245–4251.
36. Boucard, A.A., Roy, M., Beaulieu, M.E., Lavigne, P., Escher, E., Guillemette, G. & Leduc, R. (2003) Constitutive activation of the angiotensin II type 1 receptor alters the spatial proximity of transmembrane 7 to the ligand-binding pocket. *J. Biol. Chem.* **278**, 36628–36636.
37. Martin, S.S., Boucard, A.A., Clement, M., Escher, E., Leduc, R. & Guillemette, G. (2004) Analysis of the third transmembrane domain of the human type 1 angiotensin II receptor by cysteine scanning mutagenesis. *J. Biol. Chem.* **279**, 51415–51423.
38. Underwood, D.J., Strader, C.D., Rivero, R., Patchett, A.A., Greenlee, W. & Prendergast, K. (1994) Structural model of antagonist and agonist binding to the angiotensin II, AT_1 subtype, G protein coupled receptor. *Chem. Biol.* **1**, 211–221.
39. Joseph, M.P., Maigret, B., Bonnafous, J.C., Marie, J. & Scheraga, H.A. (1995) A computer modeling postulated mechanism for angiotensin II receptor activation. *J. Protein Chem.* **14**, 381–398.
40. Paiva, A.C.M., Costa-Neto, C.M. & Oliveira, L. (1998) *Molecular Modeling and Mutagenesis Studies of Angiotensin II/AT_1* Interaction and Signal Transduction. Available at: http://www.mcmaster.ca/inabis98/escher/paiva0625
41. Oliveira, L., Paiva, A.C.M. & Vriend, G. (1999) A low resolution model for the interaction of G proteins with G protein-coupled receptors [review]. *Protein Eng.* **12**, 1087–1095.
42. Horn, F., van der Wenden, E.M., Oliveira, L., Ijzerman, A.P. & Vriend, G. (2000) Receptors coupling to G proteins: is there a signal behind the sequence? *Proteins* **41**, 448–459.
43. Boucard, A.A., Wilkes, B.C., Laporte, S.A., Escher, E., Guillemette, G. & Leduc, R. (2000) Photolabeling identifies position 172 of the human AT_1 receptor as a ligand contact point: receptor-bound angiotensin ii adopts an extended structure. *Biochemistry* **39**, 9662–9670.
44. Hunyady, L., Vauquelin, G. & Vanderheyden, P.M.L. (2003) Agonist induction and conformational selection during activation of a G-protein-coupled receptor. *Trends Pharmacol. Sci.* **24**, 81–86.
45. Pebay-Peyroula, E., Rummel, G., Rosenbusch, J.P. & Landau, E.M. (1997) X-ray structure of bacteriorhodopsin at 2.5 angstroms from microcrystals grown in lipidic cubic phases. *Science* **277**, 1676–1681.
46. Palczewski, K., Takashi, K., Tetsuya, H., Behnke, C., Motoshima, H., Fox, B., Le Trong, I., Teller, D., Okada, T., Stenkamp, R., Yamamoto, M. & Miyano, M. (2000) Crystal structure of rhodopsin: a G-protein-coupled receptor. *Science* **289**, 739–745.
47. Baldwin, J.M., Schertler, G.F. & Unger, V.M. (1997) An alpha-carbon template for the transmembrane helices in the rhodopsin family of G-protein-coupled receptors. *J. Mol. Biol.* **272**, 144–164.
48. de Gasparo, M., Catt, K.J., Inagami, T., Wright, J.W. & Unger, T. (2000) International union of pharmacology: XXIII. The angiotensin II receptors [review]. *Pharmacol. Rev.* **52**, 415–472.
49. Sano, T., Ohyama, K., Yamano, Y., Nakagomi, Y., Nakazawa, S., Kikyo, M., Shirai, H., Blank, J.S., Exton, J.H. & Inagami, T. (1997) A domain for G protein coupling in carboxyl-terminal tail of rat angiotensin II receptor type 1a. *J. Biol. Chem.* **272**, 23631–23636.
50. Dunfield, L.G., Burgess, A.W. & Scheraga, H.A. (1978) Energy parameters in polypeptides: 8. Empirical potential energy algorithm for the conformational analysis of large molecules. *J. Phys. Chem.* **82**, 2609–2616.
51. Nemethy, G., Pottle, M.S. & Scheraga, H.A. (1983) Energy parameters in polypeptides: 9. Updating of geometrical parameters, nonbonded interactions, and hydrogen bond interactions for the naturally occurring amino acids. *J. Phys. Chem.* **87**, 1883–1887.
52. Nikiforovich, G.V., Galaktionov, S., Balodis, J. & Marshall, G.R. (2001) Novel approach to computer modeling of seven-helical transmembrane proteins: current progress in test case of bacteriorhodopsin. *Acta Biochim. Pol.* **48**, 53–64.
53. Nikiforovich, G.V., Hruby, V.J., Prakash, O. & Gehrig, C.A. (1991) Topographical requirements for delta-selective opioid peptides. *Biopolymers (Pept. Sci.)* **31**, 941–955.
54. Nikiforovich, G.V. (1994) Computational molecular modeling in peptide design. *Int. J. Pept. Protein Res.* **44**, 513–531.
55. Hunyady, L., Bor, M., Balla, T. & Catt, K.J. (1994) Identification of a cytoplasmic Ser-Thr-Leu motif that determines agonist-induced internalization of the AT1 angiotensin receptor. *J. Biol. Chem.* **269**, 31378–31382.
56. Auger-Messier, M., Clement, M., Lanctot, P.M., Leclerc, P.C., Leduc, R., Escher, E. & Guillemette, G. (2003) The constitutively active N111G-AT_1 receptor for angiotensin II maintains a high affinity conformation despite being uncoupled from its cognate G protein Gq/11alpha. *Endocrinology* **144**, 5277–5284.
57. Nikiforovich, G.V. & Marshall, G.R. (2001) 3D model for TM region of the AT-1 receptor in complex with angiotensin II independently validated by site-directed mutagenesis data. *Biochem. Biophys. Res. Commun.* **286**, 1204–1211.
58. Nikiforovich, G.V. & Marshall, G.R. (2003) 3D model for meta-II rhodopsin, an activated G-protein-coupled receptor. *Biochemistry* **42**, 9110–9120.
59. Mirzadegan, T., Benko, G., Filipek, S. & Palczewski, K. (2003) Sequence analyses of G-protein coupled receptors: similarities to rhodopsin. *Biochemistry* **42**, 2767–2769.
60. Nikiforovich, G.V. (1998) A novel non-statistical method for predicting breaks in transmembrane helices. *Protein Eng.* **11**, 279–283.

61. Teller, D.C., Okada, T., Behnke, C.A., Palczewski, K. & Stenkamp, R.E. (2001) Advances in determination of a high-resolution three-dimensional structure of rhodopsin, a model of G protein-coupled receptors (GPSRs). *Biochemistry* **40**, 7761–7772.
62. Okada, T., Fujiyoshi, Y., Silow, M., Navarro, J., Landau, E.M. & Shichida, Y. (2002) Functional role of internal water molecules in rhodopsin revealed by X-ray crystallography. *Proc. Natl Acad. Sci. U S A* **99**, 5982–5987.
63. Okada, T., Sugihara, M., Bondar, A.N., Elstner, M., Entel, P. & Buss, V. (2004) The retinal conformation and its environment in rhodopsin in light of a new 2.2 a crystal structure. *J. Mol. Biol.* **342**, 571–583.
64. Li, J., Edwards, P.C., Burghammer, M., Villa, C. & Schertler, G.F. (2004) Structure of bovine rhodopsin in a trigonal crystal form. *J. Mol. Biol.* **343**, 1409–1438.
65. Meng, E.C. & Bourne, H.R. (2001) Receptor activation: what does the rhodopsin structure tell us? *Trends Pharmacol. Sci.* **22**, 587–593.
66. Hubbell, W.L., Altenbach, C. & Khorana, H.G. (2003) Rhodopsin structure, dynamics and activation. *Adv. Protein Chem.* **63**, 243–290.
67. Sakmar, T.P., Menon, S.T., Marin, E.P. & Awad, E.S. (2002) Rhodopsin: insights from recent structural studies. *Annu. Rev. Biophys. Biomol. Struct.* **31**, 443–484.
68. Sheikh, S.P., Vilardarga, J.P., Baranski, T.J., Lichtarge, O., Iiri, T., Meng, E.C., Nissenson, R.A. & Bourne, H.R. (1999) Similar structures and shared switch mechanisms of the beta2-adrenoceptor and the parathyroid hormone receptor. Zn(II) bridges between helices III and VI block activation. *J. Biol. Chem.* **274**, 17033–17041.
69. Elling, C.E., Thirstrup, K., Holst, B. & Schwartz, T.W. (1999) Conversion of agonist site to metal-ion chelator site in the $beta_2$-adrenergic receptor. *Proc. Natl Acad. Sci. U S A* **96**, 12322–12327.
70. Gether, U., Lin, S., Ghanouni, P., Ballesteros, J.A., Weinstein, H. & Kobilka, B.K. (1997) Agonists induce conformational changes in transmembrane domains III and VI of the $beta_2$ adrenoceptor. *EMBO J.* **16**, 6737–6747.
71. Jensen, A.D., Guarnieri, F., Rasmussen, S.G., Asmar, F., Ballesteros, J.A. & Gether, U. (2001) Agonist-induced conformational changes at the cytoplasmic side of transmembrane segment 6 in the beta 2 adrenergic receptor mapped by site-selective fluorescent labeling. *J. Biol. Chem.* **276**, 9279–9290.
72. Porter, J.E. & Perez, D.M. (1999) Characteristics for a salt-bridge switch mutation of the $alpha_{1b}$ adrenergic receptor. Altered pharmacology and rescue of constitutive activity. *J. Biol. Chem.* **274**, 34535–34538.
73. Shapiro, D.A., Kristiansen, K., Weiner, D.M., Kroeze, W.K. & Roth, B.L. (2002) Evidence for a model of agonist-induced activation of 5-hydroxytryptamine 2a serotonin receptors that involves the disruption of a strong ionic interaction between helices 3 and 6. *J. Biol. Chem.* **277**, 11441–11449.
74. Sylte, I., Bronowska, A. & Dahl, S.G. (2001) Ligand induced conformational states of the $5\text{-}HT_{1a}$ receptor. *Eur. J. Pharmacol.* **416**, 33–41.
75. Visiers, I., Ballesteros, J.A. & Weinstein, H. (2002) Three-dimensional representations of G protein-coupled receptor structures and mechanisms. *Methods in Enzymology* **343**, 329–371.
76. Perez, D.M. & Karnik, S.S. (2005) Multiple signaling states of G-protein-coupled receptors. *Pharmacol. Rev.* **57**, 147–161.
77. Galaktionov, S., Nikiforovich, G.V. & Marshall, G.R. (2001) Ab initio modeling of small, medium and large loops in proteins. *Biopolymers (Pept. Sci.)* **60**, 153–168.